

# Detecting falls by analyzing angular momentum

Dario Martelli and Vito Monaco

BioRobotics Institute  
Scuola Superiore Sant'Anna  
Pisa, Italy  
[d.martelli@sssup.it](mailto:d.martelli@sssup.it)  
[v.monaco@sssup.it](mailto:v.monaco@sssup.it)

Silvestro Micera

BioRobotics Institute,  
Scuola Superiore Sant'Anna  
Pisa, Italy  
Institute for Automation, Swiss Federal Institute of  
Technology  
Zurich, Switzerland.  
[micera@sssup.it](mailto:micera@sssup.it)

**Abstract**— The aim of the present pilot study is to investigate the hypothesis that fall detection systems based on sensors placed on the distal segments of the body are more effective than solution based on placing sensors on the trunk. To test this hypothesis, we observed the contribution of all body segments to the 3D angular momentum. Five healthy adults were enrolled for the experimental sessions. A set of 39 spherical markers was located on body landmarks and subjects underwent perturbed walking while a Motion Analysis System recorded 3D kinematics. From a biomechanical model, the angular momentum pattern related to each body segment was estimated. Data were post-processed with a threshold-based algorithm used to detect which among body segments allows detect as soon as possible and with limited false alarms the perturbation. Results showed that hands-forearms and chest-head are the most sensitive to external moments orientated along respectively the anterior-posterior and medio-lateral directions.

**Keywords**-fall detection; movement analysis; biomechanical model; angular momentum

## I. INTRODUCTION

One of the consequences of aging is the reduced ability to maintain balance; this leads to an increased risk of falling, causing both traumatic and psychological consequences [1, 2]. Falls mainly occur at home, during daily activities, due to tripping or slipping [2, 3]. Overall, falling, in conjunction with the increased averaged age of the worldwide population, is becoming a priority issue both for the health of people and the health care system [2, 3].

Some research groups have focused their attention on incipient falling detection, in order to design wearable devices, which can mitigate the effects of a possible impact with the ground [4-9]. An effective fall detection and injury prevention system can increase the confidence and the independence of elderly and improve their quality of life. However, since fall is an unexpected, sudden, and not uniquely characterized occurrence, the design of such systems is very complex and current solutions do not fully satisfy the requirements of reliability and tolerance. In particular, fall detectors are prone to several errors and they are often only able to send a rescue message after an event recognized as “fall”. These devices are generally based on inertial sensors mounted at the belt level and compare kinematic related features (e.g., acceleration,

velocities, height, etc.) during activities of daily life to those expected during a fall [4-9]. Kinematic features related to a fall are estimated while subjects fall either passively or as a result of pushing, so in a structured work frame [4-9]. Finally, the location of these sensors is presumably influenced by aesthetic and/or ergonomic factors, which could promote their acceptability by the user.

As far as we are concerned, in order to describe real features of an incipient fall, it is important to investigate the active behavior of subjects while experiencing a sudden, unexpected perturbation of the balance during common motor tasks. In particular, the analysis of the 3D whole body biomechanics during these conditions can allow to better understanding the reactive action adopted by subjects and, consequently, to highlight whether they achieve systematic movements which can be predictive of an incipient fall. If confirmed, these insights can be used to both proactively detect a fall before the impact with the ground, and design control algorithms leading exoskeleton able to deliver supplementary forces suddenly after a perturbation to recovery balance.

Common experience, supported by scientific literature [10], consists of observing subjects caught by an unexpected perturbation while vigorously move their arms in order to recover the balance. This experience would suggest a different approach to the location of the inertial sensors. In particular, it is possible to hypothesize that distal segments can more readily detect incipient falling event than the trunk.

The present pilot study aims at investigating the hypothesis that a fall detector based on sensors placed on the distal segments of the body is more effective than solutions based on sensors located on the trunk. To test this hypothesis, we needed to adopt a metric sensitive to the variation of stability, and allowing analyzing the contribution of all individual body segments while recovering balance control after a perturbation. In this regard, since the Whole Body Angular Momentum (WBAM) accounts for the contributions of all individual segments and is directly reflected into the dynamical stability during many motor tasks [11-13], it was adopted as main metric to analyze the behavior of healthy subjects while experiencing an unexpected perturbation during locomotion. In particular it was investigate which, among body segments,

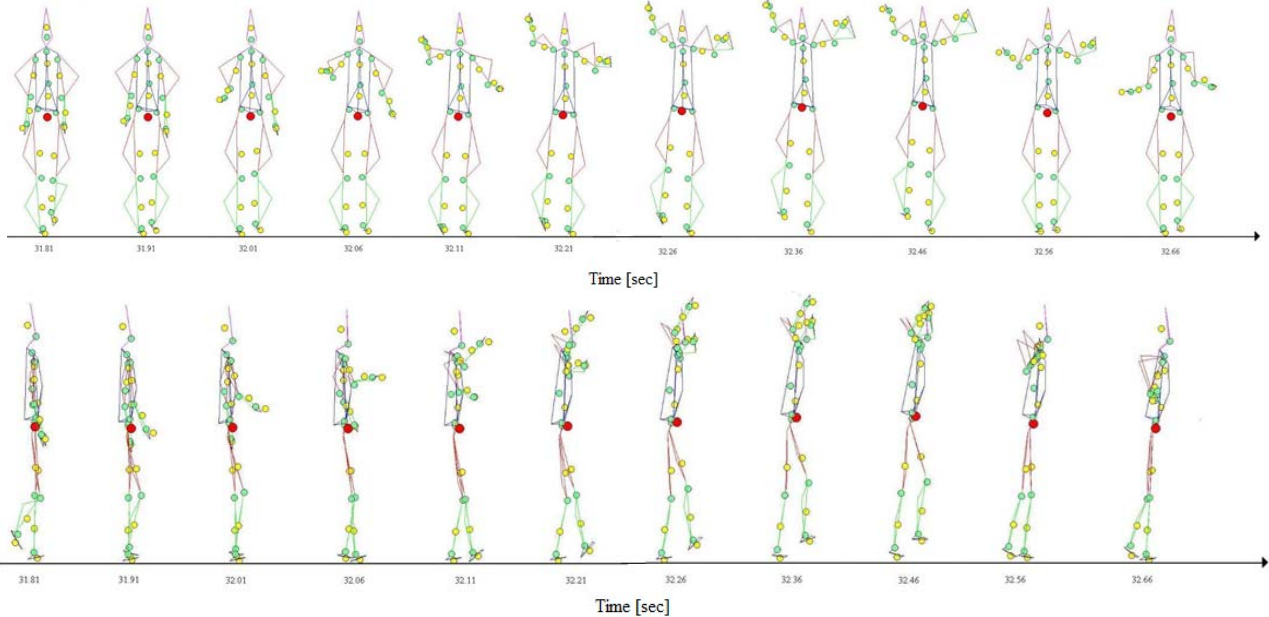


Figure 1. Top and bottom sequences respectively represent the frontal and the lateral view of a subject while experiencing a forward towards outside sliding of the right foot (NE\_R perturbation). Vertices of polygons reflect the position of markers in space, green circles represent the articular joints, yellow circles represent the position of the center of mass of all body segments, the red circle represents the whole body center of mass.

allow to correctly identifying as soon as possible the subject response to a destabilization.

## II. MATERIAL AND METHODS

### A. Experimental procedures

Five healthy adults (3 male and 2 females,  $26.0 \pm 0.9$  years old,  $61.2 \pm 11.7$  kg,  $1.700 \pm 0.075$  m, right-handed), were enrolled for the experimental sessions. A set of 39 spherical markers (diameter: 14 mm) was located on body landmarks. Markers were attached on: vertex, left and right gonions, for the head; clavicle, sternum, C7 vertebrae, and acromions, for the upper trunk; lateral epicondyle of the humerus, radial styloids, ulnar styloids, third metacarpal bones and additional markers rigidly attached to wands over the mid-humerus, for both arms; sacrum, left and right anterior superior iliac spines, for the pelvis; prominence of the greater trochanter external surface, lateral epicondyle of the femur, heads of fibula, lateral malleolus, calcaneus, first and fifth metatarsal heads, tip of the toes, and additional markers rigidly attached to wands over the mid-femur and mid-shaft of the tibia, for both the legs.

Before trials, a static calibration procedure was carried out for each subject placing 7 additional markers on T10 vertebrae, for the upper body; medial epicondyle of the humerus, for both arms; medial epicondyle of the femur and medial malleolus, for both legs. This procedure was basically used to define the biomechanical model of the subject in accordance with the literature [14, 15]. The walking speed for each subject was chosen according to the Froude number (Fr) [16]. In this study was chosen  $Fr=0.15$ . Subjects underwent perturbed locomotion while the 3D kinematics was recorded by means of a 6-camera based Vicon 512 Motion Analysis System (Oxford, UK) with a sample rate of 100 Hz.

Perturbations were managed by SENLY, a mechatronic platform, result of a collaboration between Tecnalia Italy and Scuola Superiore Sant'Anna shown in Figure 2 [17]. It mainly consists of two parallel and adjacent treadmills, in which speed profile of both longitudinal and transversal directions can be independently controlled. In this way it was possible to apply slipping perturbations in the horizontal plane by means of sudden movements of one or both treadmills. The experimental protocol accounted for 10 types of perturbations, 5 on the left foot and 5 on the right foot, each involving the combination of longitudinal (North, N or South, S) and transversal (East, E, or West, W) movements of the treadmill, provided twice for each subject. Herein, perturbation will be named with acronyms indicating perturbed foot (L: left; R: Right) and direction of the perturbation: N\_R, NE\_R, E\_R, SE\_R, S\_R, N\_L, NW\_L, W\_L, SW\_L, S\_L. In order to adopt a standard framework for



Figure 2. SENLY platform.

all subjects, perturbations were run when the early stance was triggered by analyzing real-time ground reactions forces. Ten further trials, without applying any perturbation were also included into the experimental protocol. To obtain reliable results, for each of the thirty trials, subjects did not know if they would have been perturbed or not.

### B. Biomechanical Model

The global right-handed reference frame was located in the center of SENLY with  $X$  axis along the anterior/posterior direction,  $Y$  axis vertical and  $Z$  axis defined by the right-hand rule, in accordance with ISB recommendations [18]. A full body model accounting for 15 segments and 42 internal degrees of freedom was realized. The 15 segments of the model were: head/neck, chest, abdomen/pelvis, upper arms, forearms, hands, thighs, legs and feet. All joints were approximated as spherical and were located in accordance with previous studies [19-22]. For the  $i^{th}$  body segment, a right-handed local reference frame was located in its own center of mass. The  $X_i$  axis was anteriorly oriented, the  $Y_i$  axis was oriented from the distal to the proximal joint, and the  $Z_i$  axis was defined by the right-hand rule, in accordance with ISB recommendations [18].

Body segment inertial parameters (mass, center of mass, height and moment of inertia tensor) were calculated using the procedures detailed by Zatsiorsky and Seluyanov [23] and modified by de Leva [24]. Missed kinematic data were estimated by means of a cubic spline interpolation. Then, the

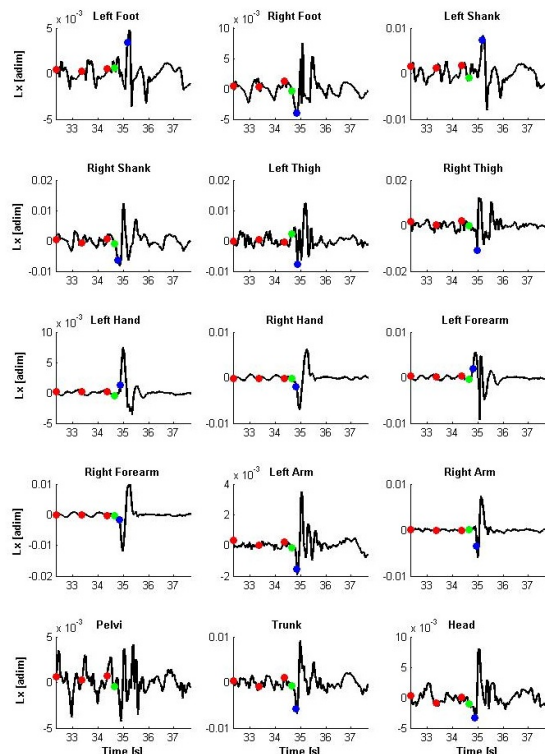


Figure 3. Antero-posterior (X) component of individual segment angular momenta (SAM), red circles represent right heel strikes, the green circle the instant of perturbation, and the blue circle the instant of detection.

whole data record was filtered by a zero-lag, 4<sup>th</sup> order Butterworth low-pass filter with cut-off at 10 Hz.

According to literature [11-13], body model and kinematics were used to estimate the individual segmental angular momenta (SAM) about the body's center of mass. Moreover, in order to reduce data variance, SAM was normalized dividing it by the product of subject's mass, height and walking speed [11-13].

### C. Incipient fall detecting

The contribution of each segment to the WBAM was analyzed by a threshold algorithm [25]. This was aimed at investigating which segment allowed recognizing as soon as possible the perturbation. Briefly the algorithm is based on the estimation of mean and standard deviation of the signal during walking trials for every subject. During perturbed trials the mean value of the signal within a moving time window  $W$  was estimated. If the mean value of the signal exceeds of  $d$  times the standard deviation obtained during walking trials, perturbation is detected. The width  $W$  of the window ( $W = 0.05$  s), and the number of standard deviations  $d$  ( $d = 4$ ) were chosen in accordance with trial-and-error tests, described in a previous work [26]. When the algorithm was able to detect the perturbation, it allowed to estimate the time elapsed from the onset of the perturbation to its detection. Otherwise it returned a false alarm (FA).

The analysis was conducted by computing an average among results obtained from all subjects and considering each

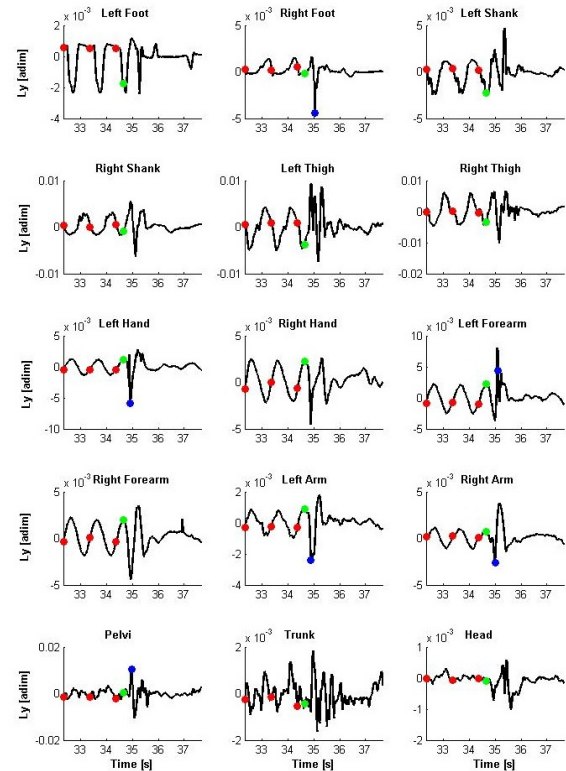


Figure 4. Vertical (Y) component of individual segment angular momenta (SAM), red circles represent right heel strikes, the green circle the instant of perturbation, and the blue circle the instant of detection.

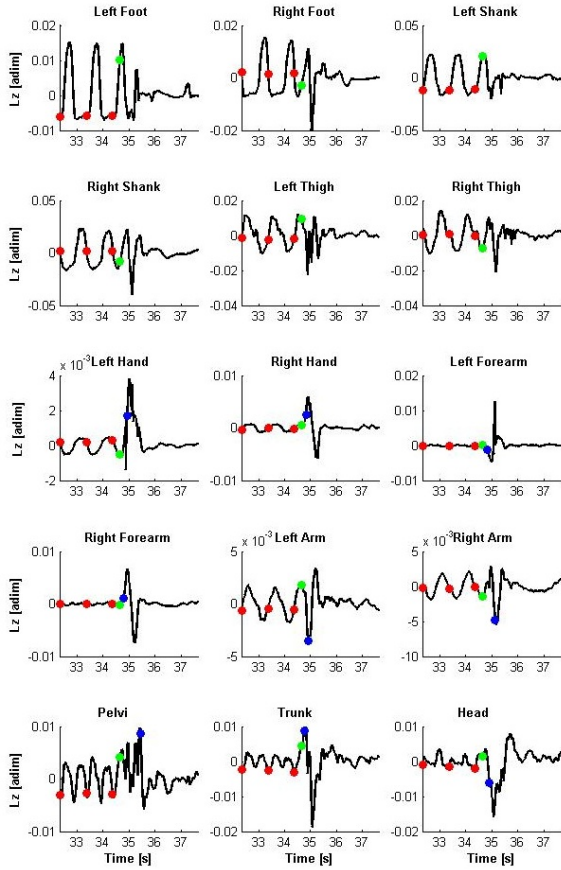


Figure 5. Medio-lateral (Z) of individual segment angular momenta (SAM), red circles represent right heel strikes, the green circle the instant of perturbation, and the blue circle the instant of detection.

type of perturbation separately. Data analysis was carried out off line by means of customized MATLAB (The MathWorks Inc., Cambridge, MA, US) scripts.

### III. RESULTS

Subjects walked on average at  $1.10 \pm 0.07$  m/s (range: 1.02–1.21 m/s). Figure 1 shows frontal and lateral views concerning the temporal evolution of the biomechanical model while

undergoing a NE\_R perturbation. It was chosen to representatively depict the behavior of a subject from the instant when the perturbation occurs up to about 1 second later. Each body segment is represented by polygons, whose vertices reflect the marker position in 3-D space. The sliding of the foot causes a forward displacement of the center of mass of the body and a back rotation of the upper body. If the subject does not respond in time to the perturbation it would face a back fall. Conversely, the subject reacts in time regaining the balance: the right arm rises quickly at first, followed immediately by the left and the other segments. Therefore, the perturbation caused significant changes on the dynamical stability and kinematics of the subject, affecting AM pattern of all segments. Figures 3, 4 and 5 show a representative example of patterns of X, Y and Z components of the AM for the same subject undergoing the perturbation reported in Figure 1.

Data referring to the time window starting two strides before and ending three seconds after the perturbation were processed by the detecting algorithm. Figure 3 shows that segments, which X component of the AM pattern were characterized by the most significant change, are those of the upper limbs (hands, forearms and arms). Their reaction takes place immediately after the perturbation. In particular, forearms showed the greater relative variation of the peak in 0.3 seconds from the perturbation. The other segments showed only slight modifications of their AM patterns. Figure 4 shows that segments underwent low and slow changes of the Y component of the AM due to the perturbation. Figure 5 shows that segments of the lower limbs and pelvis are not affected by the perturbation, whereas right upper limb, chest, and head had a significantly variation of the Z component of the AM.

Figure 6 reports boxplots concerning the output of the algorithm in term of number of body segments characterized by a significant modification of their AM patterns. The non-parametric Friedman test allowed us to reject the hypothesis that results of the algorithm belonged to the same population ( $p < 0.01$  with respect of both components of the AM and directions of perturbation). In particular, concerning AM components, since the Y one appeared less sensitive to the perturbation, it was considered not suitable for fall detection.

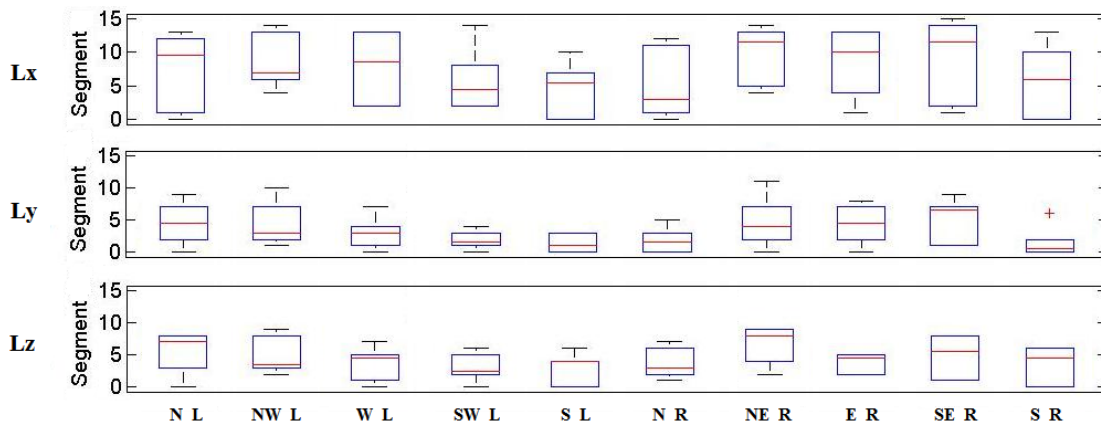


Figure 6. Boxplots concerning the output of the algorithm in term of number of body segments characterized by a significant modification of their AM patterns. The x-axis represents the 10 types of perturbations. The y-axis represents the number of body segments.

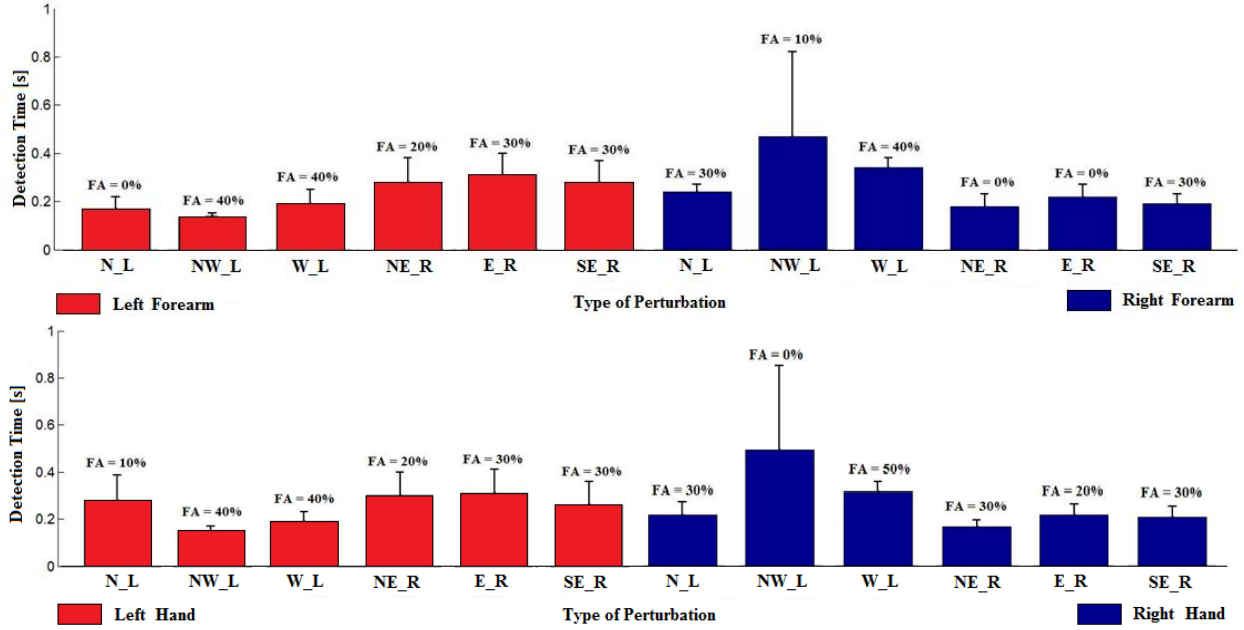


Figure 7. Bar graphs represent threshold algorithm performances related to forearms and hands X component of AM. The x-axis represents the remaining 6 types of perturbations. The y-axis represents the time elapsed between the perturbation and the detection of it. The percentage of FA are positioned upon the bars. Red and blue bars represents respectively results of left and right segments.

Moreover, with respect to the adopted perturbations, N\_R, S\_R, SW\_L and S\_L appeared to slightly modify angular momentum patterns such that the detecting algorithm was able to correctly individuate the disabling occurrences in few segments. For these reasons, further analyses have been carried out only for the remaining components and perturbations because they appeared more prone to significantly modify body

dynamics.

The sensitivity of the detecting algorithm was analyzed in term of detection time and percentage of false alarms (FAs). Results showed that data referring to forearms, hands, chest, and head were those allowing the best solution [26]. Therefore, we analyzed data performance related to these body segments (Figures 7 and 8). In particular, body segments allowing for the best results due to the analysis of the X component of the AM were hands and forearms (Figure 7). Moreover, it was observed a bias related to the laterality of the perturbation. For instance, right perturbations were quickly detected on the right limbs. Concerning the medio-lateral component, the detecting algorithm was characterized by the best performance while processing data related to the chest and head (Figure 8).

#### IV. DISCUSSION

Current systems for the detection of falls often use algorithms comparing kinematic features during daily activities to those related to simulated fall [4-10]. Moreover, sensor location is presumably influenced by aesthetic and/or ergonomic factors, which could promote their acceptability by the user. Our goal was to investigate whether it is possible to find an optimal location for these sensors based on the sensitiveness of body segments while an external perturbation destabilizes the balance control. Noticeable, our purpose is to identify the perturbation as soon as possible, in order to enable proactive actions aimed at compensating the lack of balance and/or mitigating the impact with the ground. Moreover, since this work is a preliminary study that aims at determining if the new methodology has some physiological relevance, we decided to only investigate healthy young subjects. After that

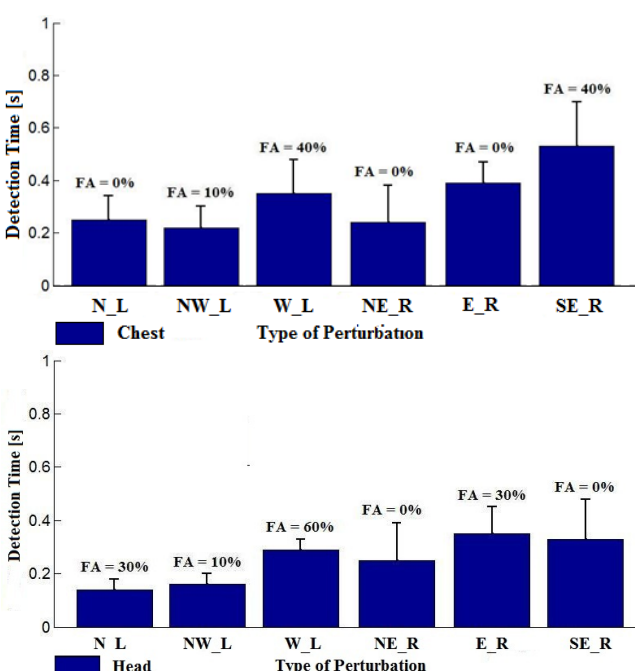


Figure 8. Bar graphs represent threshold algorithm performances related to chest and head Z component of AM. The x-axis represents the remaining 6 types of perturbations. The y-axis represents the time elapsed between the perturbation and the detection of it. The percentage of FA are positioned upon the bars.

we will consider the elderly people, who are the real target of the research.

The analysis of the trend of all components of the normalized AM related to each segment during perturbed walking tests (see Figure 3, 4, 5) showed that upper limb segments are very sensitive to sudden variation of the balance. It highlights that, due to a perturbation, subjects tend to maintain balance by a sudden reaction of upper limbs. In particular, rapid movements of upper limbs can suitably manage the balance with respect the antero-posterior and medio-lateral moment generated by external perturbations.

With respect to destabilizing vertical moments, we observed that body segments did not show significant modifications of the AM patterns (Figures 4 and 6). This was presumably due to the fact that adopted perturbations did not significantly affect the balance with respect to the yaw of the body because they consisted in mono-directional planar movement of the belt. Therefore, this component cannot be considered to detect perturbations as those adopted in this study.

Another result observed after fall detecting analysis, was that some perturbations modify AM patterns only in a few segments (Figure 6). Concerning perturbations directed to the backward direction, we believe that they can be easily managed by a further step, which mainly modifies the dynamics of locomotion increasing gait velocity. Concerning the N\_R perturbation, it is possible to hypothesize that the dominance of subjects (e.g., right-handed) may have affected their biomechanical response. Further analysis required to deeply investigate this latter argument.

According to these results, we can conclude that hands and forearms (Figure 7) are the most suitable segments to detect balance perturbations due to external moments applied along the antero-posterior direction. Moreover, chest and head (Figure 8) are the segments mainly used to balance external moments along the medio-lateral direction. This strategy appears to be physiologically consistent with the body stiffness in the frontal and the sagittal planes. In particular, since the body stiffness in the frontal plane is greater than that in the sagittal one, the enrollment of upper limbs can be considered enough in order to compensate the variation of the antero-posterior component of the whole body AM. Accordingly, movements of the trunk are necessary to compensate the variation of the medio-lateral component of the whole body AM. This is because the lower stiffness of the body in the sagittal plane allow greater velocities and, consequently, greater variations of the AM which need to be compensated by a stronger action. In this regard, the trunk, due to its greater inertia, can suitably achieve this goal. However, it is important to remark that, due to their low inertia, upper limb related responses are the quickest among all body segments.

Actually, the laterality of the perturbations affects in a significant way the segments involved in the balance recovery. In fact, when perturbations were right oriented, the right side of subjects reacted quicker than the contralateral one and vice

versa. This behavior should be accounted for a fall detection system, involving sensors located on both sides of the body. This means that fall detecting system should account for the integration of more redundant sensors located on both upper distal segments (e.g., at the level of the wrists) and upper trunk (e.g., at the level of the neck) in order to improve the sensitiveness of the system. This would hence avoid false positives due to daily activities reducing unexpected response of systems leaded by the proposed algorithm.

## V. CONCLUSION

This preliminary study provides guidelines concerning an appropriate positioning of sensors related to fall detection based on the analysis of the AM. Results seem to support the hypothesis that placing sensors on both upper distal segments of the body (e.g., at the level of the wrists) and on the upper trunk (e.g., at the level of neck) can significantly increase the performance of system for fall detection. Nevertheless, at the moment, the percentage of false alarms is too high to use presented approach. Therefore, further investigations are needed to enhance the performance and integrate the response of more segments.

## REFERENCES

- [1] M. Pijnappels, J.C.E. van der Burg, N.D. Reeves, and J.H. van Dieën, "Identification of elderly fallers by muscle strength measures," *Eur J Appl Physiol*, vol. 102, pp. 585–592, 2008.
- [2] T. Masud, and R.O. Morris, "Epidemiology of falls," *Age and Ageing*, vol. 30, pp. 3-7, 2001.
- [3] E.T. Hsiao-Wecksler, "Biomechanical and age-related differences in balance recovery using the tether-release method," *Journal of Electromyography and Kinesiology*, vol. 18, pp. 179–187, 2008.
- [4] G. Wu, "Distinguishing fall activities from normal activities by velocity characteristics," *J Biomech*, vol. 33, no. 11, pp. 1497–1500, 2000.
- [5] G. Wu and S. Xue, "Portable Preimpact Fall Detector With Inertial Sensors," *IEEE Transactions on neural systems and rehabilitation engineering*, vol. 16(2), april 2008.
- [6] A.K. Bourke, and G.M. Lyons, "A threshold-based fall-detection algorithm using a bi-axial gyroscope sensor," *Medical Engineering and Physics*, vol. 30(1), pp. 84–90, 2008.
- [7] M.N. Nyan, F.E.H. Tay, A.W. Tan, and K.H. Seah, "Distinguishing fall activities from normal activities by angular rate characteristics and high-speed camera characterization," *Medical Engineering & Physics*, vol. 28(8), pp. 842–849, 2006.
- [8] M.N. Nyan, F.E.H. Tay, and E. Murugasu, "A wearable system for pre-impact fall detection," *J Biomech*, vol. 41, pp. 3475–3481, 2008.
- [9] M.N. Nyan, F.E.H. Tay, and M.Z.E. Mah, "Application of motion analysis system in pre-impact fall detection," *J Biomech*, vol. 41(10), pp. 2297–2304, 2008.
- [10] M. Pijnappels, I. Kingma, D. Wezenberg, G. Reurink, and J.H. van Dieën, "Armed against falls: the contribution of arm movements to balance recovery after tripping," *Exp Brain Res*, 2010 Apr;201(4):689–99. Epub, Decembre 1, 2009.
- [11] H. Herr, and M. Popovic, "Angular momentum in human walking," *J Exp Biol*, vol. 211, pp. 467–481, 2008.
- [12] B.C. Bennett, S.D. Russell, P. Sheth, and M.F. Abel, "Angular momentum of walking at different speeds," *Hum Mov Sci*, vol. 29, pp. 114–124, 2010.
- [13] T. Robert, B.C. Bennett, S.D. Russell, C.A. Zirker, and M.F. Abel, "Angular momentum synergies during walking," *Exp Brain Res*, vol. 197, pp. 185–197, 2009.

- [14] P. Allard, A. Cappozzo , A. Lundberg , and C.L. Vaughan, "Three dimensional analysis of human locomotion," vol. 2, ed. Chichester: John Wiley & Sons Inc., pp. 173–189, 1997.
- [15] D.A. Winter, "Biomechanics and motor control of human movement", 3rd ed., New Jersey: John Wiley & Sons Inc., 2005.
- [16] C.L. Vaughan, M.J. O'Malley, "Froude and the contribution of naval architecture to our understanding of bipedal locomotion," *Gait Postur.*, vol. 21, pp. 350-362, 2005.
- [17] E. Cattin, L. Bassi Luciani, V. Genovese, V. Monaco, G Macri, L. Odetti, S. Micera., "SENYL: a novel robotic platform for fall risk prevention", Workshop ICRA 2010.
- [18] G. Wu, and P.R. Cavanagh, "ISB recommendations for standardization in reporting of kinematic data", *J Biomech*, vol. 28, no. 10, pp. 1257-1261, 1995.
- [19] X.G. Wang, "Construction of arm kinematic linkage from external surface markers," in: Proceedings of the Fourth International Symposium on 3D Analysis of Human Movement, Grenoble, France, 1996.
- [20] C. Anglin, and U.P. Wyss, "Arm motion and load analysis of sit-to-stand, stand-to-sit, cane walking and lifting," *Clin Biomech*, vol. 15, pp.441-448, 2000.
- [21] A.L. Bell, D.R. Pedersen, and R.A. Brand, "A comparison of the accuracy of several hip center location prediction methods," *J Biomech*, vol. 23, no. 6, pp. 617-621, 1990.
- [22] R.B. Davis III, S. Öunpuu, D. Tybursky, and J.R. Gage, "A gait analysis data collection and reduction technique," *Hum Mov Sci*, vol. 10, pp. 575-587, 1991.
- [23] V.M. Zatsiorsky, V.N. Seluyanov, and L.G. Chugunova, "Methods of determining mass-inertial characteristics of human body segments," in *Contemporary Problems of Biomechanics*, pp. 272-291, 1990.
- [24] P. de Leva, "Adjustments to Zatsiorsky-Seluyanov's segment inertia parameters," *J Biomech*, vol. 29( 9), pp. 1223-1230, 1996.
- [25] P.W. Hodges and B.H. Bui, "A comparison of computer-based methods for determination of onset of muscle contraction using electromyography," *Electroenceph.Clin.N europhysiol.*, vol. 101, pp. 511–519, 1996.
- [26] D. Martelli, "Caratterizzazione del rischio di caduta mediante l'uso di un sistema meccatronico perturbativo", Master's degree thesis, December 2010.